



Article

The Effect of the Support Mass in 3D Printing on the Forming Time of the Model

Zhenjie Liang¹, Yifan Xie¹, Yining Zhang¹, Guanyixuan Zhao¹, Qifeng Lin¹, Dapeng Zhang^{1,*}, Haoyu Jiang²

¹ Ship and Maritime College, Guangdong Ocean University, Zhanjiang 524005 China

² School of Electronics and Information Engineering, Guangdong Ocean University, Zhanjiang 316021, China

Academic Editor: Weiwei Wang <zhwangww@ytu.edu.cn>

Received: 1 May 2024; Revised: 12 May 2024; Accepted: 17 May 2024; Published: 17 May 2024

Abstract: 3D printing technology has a very wide range of applications in various fields, when rapid manufacturing and chain stability are required in production; 3D printing technology can fulfil both conditions. However, limited by printer specifications, medium to large components must be printed in sections. For the quality of the products it is sometimes necessary to adjust the angle of placement of the model, these will affect the time it takes to print the model. In this paper, we will investigate the intricate interplay between support mass and printing time, tilt angle and support mass, as well as tilt angle and forming time, utilizing two distinct 3D printing technologies: FDM and UV-Curing. Furthermore, we aim to compile comprehensive data tables and line graphs to provide a visual representation of our findings. This paper hope to provide insights into the further development of 3D printing for the manufacture of medium to large parts and promote their wider application and research in various fields.

Keywords: 3D printing; Angle of placement; Support mass

1. Introduction

With the development of technology and economy, industrial products are not only a necessity for people, but also play a very important role in maintaining the stability of the society and even the country. Therefore, the stability of the production of industrial products is particularly important, and the emergence of 3D printing technology has brought a better solution to this problem. Traditional manufacturing produces products by cutting, trimming, thwarting, and other material reduction methods, this process will generates a lot of material

Citation: Liang Z., Xie Y., Zhang Y., Zhao G., Lin Q., Zhang D., Jiang H. The Effect of the Support Mass in 3D Printing on the Forming Time of the Model. Eng. Solut. Mech. Mar. Struct. Infrastruct., 2024, 1(2), doi: 10.58531/esmmsi/1/2/7

ISSN/© By the Author(s) 2024, under the CC BY-NC-ND license (<http://creativecommons.org/licenses/by-nc-nd/4.0>)

waste; moreover, the production process sometimes generates a large amount of dust, which enters the lungs by the respiratory tract and causes some damage to the human body. Human-dependent manufacturing is highly susceptible to biological factors, such as the COVID-19; which leads to instability in the production chain. And 3D printing technology is also called additive manufacturing [1], The final product is obtained by layering materials on top of each other; this process greatly reduces material wastage and ensures the stability of the production chain. 3D printing technology has a wide range of applications in architecture, aerospace, biomedicine and many other fields, printing materials such as metals, ceramics, photosensitive resins, food materials and so on [2]. Contributed greatly to the field of materials research in the field of shipbuilding and research on offshore structures. [3-5]. The Oak Ridge National Laboratory's Manufacturing Demonstration Facility and the U.S. Navy's Destructive Technology Laboratory collaborated on the first military-printed 3D submarine shell [6] in 2017. The oceans, as the vast expanse of the earth, are rich in resources waiting to be exploited; the construction of ships and offshore platforms is necessary for the exploration of the oceans [7]. Due to the limitations of current technology, the maximum space that can be moulded by today's 3D printers is a square with a side length of 12m. Meng lei Mei, Qi Qin and others segment printing method proposed to provide ideas for large ship construction, they were also used the software to investigate the relationship between the amount of support added to the hull of a segmentally printed ship and the printing time [8]. With reference to this research methodology, this paper will delve deeper into the effect of multiple variables on printing time by controlling variables and increasing or decreasing the support mass by changing the angle of the model's placement, we propose some suggestions and reference methods for the future 3D printing of producing medium and large components, ship models and other fields.

2. Software and 3D Printers Will be Needed.

2.1 Modelling Software: Solidworks;3ds Max

Both types of software are used to build 3D models, and both types of them have their advantages and disadvantages. 3ds Max is easier and simpler than solidworks for surface design. Solidworks [9-10] has a great advantage in parts, mechanical design, parts assembly, the software can easily use multiple custom planes to split the 3D model into multiple parts, so we will use 3ds Max [11] to model the model and solidworks to split it. STL format is the common "language" of slicing software and 3D modelling software [12], 3ds Max builds the model and then exports it to STL format and then uses solidworks to import it.

2.2 Slicing Software: Bambu Studio; CHITUBOX

The principle of slicing software is to convert a digital 3D model into a code can be recognised by the 3D printer and then execute that code on the 3D printer. Generally speaking, different slicing software corresponds to different types of 3D printers, but some of them are common, Bambu Studio for FDM printers, CHITUBOX for light-curing printers.

2.2.1 Fused Deposition 3D Printer (FDM)

FDM, was also named Fused Filament Fabrication (FFF), is an additive manufacturing process that belongs to the material extrusion series [13]. During operation, thermoplastic materials [14], including acrylonitrile-butadiene-styrene terpolymer (ABS), polylactic acid (PLA), polycarbonate (PC), and others, are heated to a melting temperature within the nozzle of the Fused Deposition Modeling (FDM) printer. Under the influence of gravity, the melted thermoplastic gracefully drips from the nozzle, landing precisely on the print bed. Guided by the slicing software, the nozzle traces a preplanned three-dimensional path, following the code until the print is flawlessly completed.

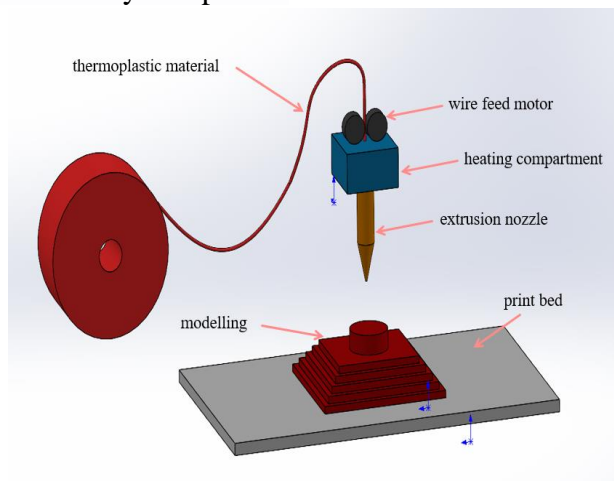


Figure. 1.FDM working sketch

2.2.2 Light-Curing 3D Printers (UV-Curing 3D Printing)

The core principle of light-curing 3D printing [15] technology lies in the selective curing of photosensitive resin [16], encompassing high-temperature-resistant resins like H100, ABS high-strength resins such as A200 eResin-ABS Pro, and versatile rigid resins known as Standard Resin. This curing process is achieved through the application of ultraviolet light, precisely controlled by digital signals. The cured resin builds up layer by layer until a complete model is formed, photosensitive resins have become the material of choice for 3D printing of high-precision products due to their excellent fluidity and instantaneous light-curing properties [17].

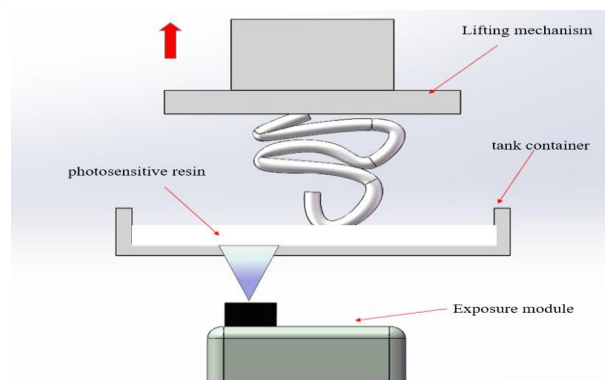


Figure. 2. Light-curing 3D printers working sketch

3. Build and Segment Models

This article will model part of the hull for research purposes, only the hull shell and part of the superstructure will be modelled. Firstly, we use 3ds Max to build the overall model, and then use solidworks to divided it into A, B, C three parts; divided out of each part are saved as a separate file (STL format). We import the file into the slicing software [18] and we can zoom in and out of the model, change the material, add supports and other parameters that you want to change in the model. Once the model has been processed in the slicing software, the file can be loaded into the 3D printer to begin the printing process.

Currently, there exists a plethora of industrial design software capable of meeting a wide range of design needs. However, the transition from modeling to configuring various parameters in slicing software is currently a manual process. If artificial intelligence were to be employed to seamlessly integrate these three processes—modeling, slicing, and printing—leaving humans only to articulate their requirements, it would undoubtedly signify a significant advancement for the manufacturing industry. This endeavor necessitates extensive employment of machine learning techniques like Physical Information Neural Networks (PINNs) [19] and the accumulation of substantial experimental data. For instance, understanding the fluid properties of thermoplastic materials as they melt or the physical effects of the flow of photosensitive resin during the light curing process. These challenges call for expertise in fluid mechanics [20-21], including Computational Fluid Dynamics.

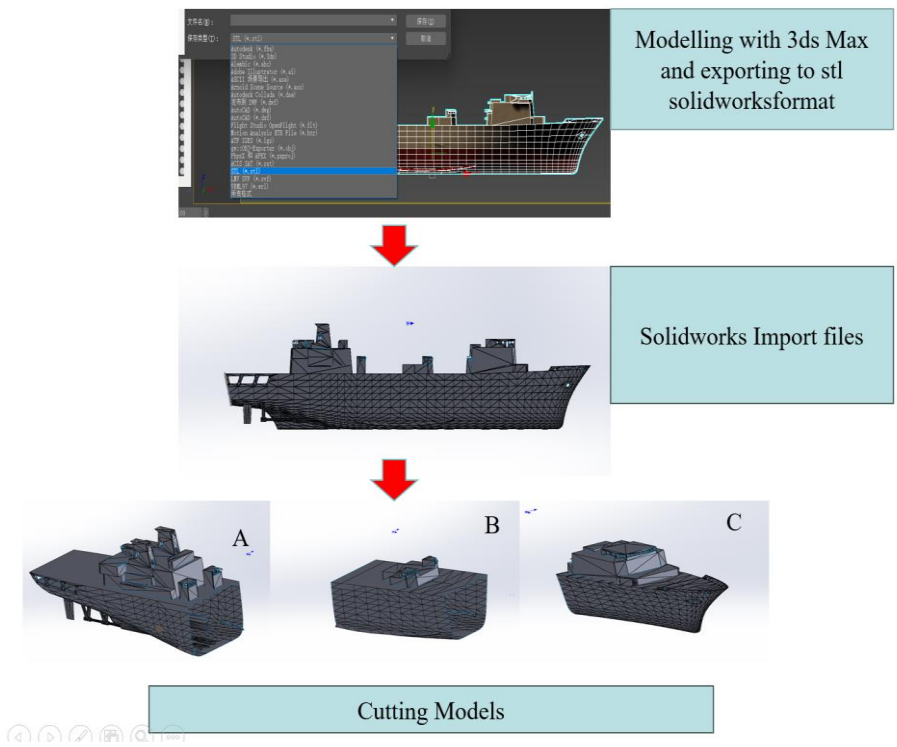


Figure 3. Modelling and cutting

4. Relevant Size Data

Table 1. Representation of physical quantities

Letters used to represent	Meaning
---------------------------	---------

V	volume
M	Mass
T	Time
K	Percentage of reduction and magnification
θ	Tilt Angle
L	Length

The physical quantities indicated in Table 1 above, as illustrated in Fig. 3, utilize $L(0)_{max}$, $W(0)_{max}$, and $H(0)_{max}$ to represent the dimensions of the model at its longest, widest, and highest points when uncut, respectively. $V(0)$ denotes the overall volume of the model. Additionally, $L(A)_{max}$, $W(A)_{max}$, $H(A)_{max}$, and $V(A)$ represent the corresponding dimensions of part A, while $L(B)_{max}$, $W(B)_{max}$, $H(B)_{max}$, and $V(B)$ are used for part B, and $L(C)_{max}$, $W(C)_{max}$, $H(C)_{max}$, and $V(C)$ for part C.

$$e + n = 10^n \tag{1}$$

Where n is a natural number, the numerical value on the right-hand side of the equation is 10^8 for $n = 8$.

4.1 Original Dimensional Parameters of Each Model

$$L(0)_{max} = 178499 \text{ mm}, \quad W(0)_{max} = 25284.5 \text{ mm}, \quad H(0)_{max} = 32026.4 \text{ mm}, \\ V(0) = 5.71265(e+13) \text{ mm}^3.$$

Part A:

$$L(A)_{max} = 71862 \text{ mm}, \quad W(A)_{max} = 24800.3 \text{ mm}, \quad H(A)_{max} = 32026.4 \text{ mm}, \\ V(A) = 2.43991(e+13) \text{ mm}^3.$$

Part B:

$$L(B)_{max} = 44243.9 \text{ mm}, \quad W(B)_{max} = 25285.5 \text{ mm}, \quad H(B)_{max} = 22227.2 \text{ mm}, \\ V(B) = 1.81837(e+13) \text{ mm}^3.$$

Part C:

$$L(C)_{max} = 62428.1 \text{ mm}, \quad W(C)_{max} = 24437 \text{ mm}, \quad H(C)_{max} = 28476.7 \text{ mm}, \\ V(C) = 1.46692(e+13) \text{ mm}^3.$$

The above data are shown in Table 2 below:

Table 2. Raw and dissected model data.

	L_{max}	W_{max}	H_{max}	V
Raw model	178499 mm	25284.5 mm	32026.4 mm	$5.71265(e+13) \text{ mm}^3$
Part A	71862 mm	24800.3 mm	32026.4 mm	$2.43991(e+13) \text{ mm}^3$
Part B	44243.9 mm	25285.5 mm	22227.2 mm	$1.81837(e+13) \text{ mm}^3$
Part C	62428.1 mm	24437 mm	28476.7 mm	$1.46692(e+13) \text{ mm}^3$

Selecting $K=1/800$, the reduced parameter sizes are shown in Table 3 below:

Table 3. $K=1/800$ model data

	L_{max}	W_{max}	H_{max}	V
Raw model	223.12375 mm	31.6056 mm	40.033 mm	111575 mm^3
Part A	89.8275 mm	31.0004 mm	40.033 mm	47654.6 mm^3
Part B	55.3049 mm	31.6069 mm	27.784 mm	35515.1 mm^3

Part C	78.0351 mm	30.5462 mm	35.5959 mm	28650.8 mm ³
--------	------------	------------	------------	-------------------------

4.2 Analysis the Difference

4.2.1 When K=1

$$L(A)_{\max} + L(B)_{\max} + L(C)_{\max} = 178534 \text{ mm} > L(0)_{\max} = 178499 \text{ mm} \quad (2)$$

Difference: $\Delta L = 35 \text{ mm}$ compared to the original model.

$$V(A) + V(B) + V(C) = 5.7252 (e+13) \text{ mm}^3 > V(0) = 5.71265 (e+13) \text{ mm}^3 \quad (3)$$

Volume difference: $\Delta V = 0.01255 (e+13) \text{ mm}^3$

Theoretically, the sum of the lengths of parts A, B, and C should match the original model's dimensions, and their combined volume should also be equal. However, currently, the combined length of parts A, B, and C exceeds the original model's length by 35mm, and their combined volume surpasses the original model's by 0.01255e+13 (mm³). This translates to an approximate length error rate of 0.0196 per cent and a volume error rate of about 0.2197 per cent.

4.2.2 After Shrinking 800 Times

$$L(A)_{\max} + L(B)_{\max} + L(C)_{\max} = 223.1675 \text{ mm} > L(0)_{\max} = 223.12375 \text{ mm} \quad (4)$$

Difference: $\Delta L = 0.04375 \text{ mm}$

$$V(A) + V(B) + V(C) = 111820.5 \text{ mm}^3 > V(0) = 111575 \text{ mm}^3 \quad (5)$$

Volume difference: $\Delta V = 245.5 \text{ mm}^3$, the length error rate is 0.0196 per cent and the volume error rate is about 0.22 per cent.

4.2.3 STL Format Mechanism

The STL format [22-24] stores part information by creating numerous triangular facets on its surface, with the accuracy of the model determined by the quantity of these facets. However, varying software applications can produce different numbers of facets when converting the same part to STL, even with identical settings. In this experiment, models A, B, and C are derived from the original and saved separately in STL format. A comparison reveals deviations in the number of facets and other parameters compared to the original, resulting in errors in length and volume. We find that there are deviations in the number of triangular facets and other parameters for a given tilt angle, but the difference in printing time is not significant; so we can ignore these effects.

5. Relationship Between the Amount of Added Support and the Forming Time of the Model (FDM)

5.1 Change the Angle of Model Placement

A model with more overhangs needs support before it can be printed [25-26]. The greater the number of overhangs, the more support is required. By adjusting the angle of the model in the slicing software, it's possible to alter the extent of overhangs and consequently, the amount of support needed. The mass of the support can be calculated by subtracting the mass of the unsupported model from the total mass of the model with added support. This mass measurement is used to determine the volume of support required.

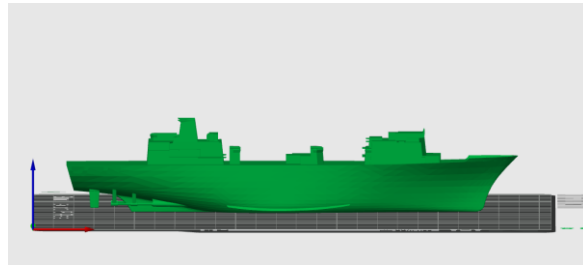


Figure 4. Models with a tilt angle of 0°

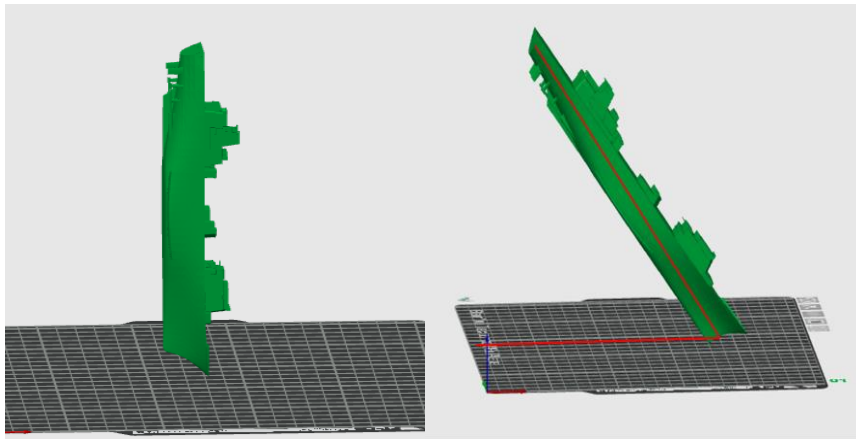


Figure 5. Models with a tilt angle of 90°

Figure 6. Models with a tilt angle of θ

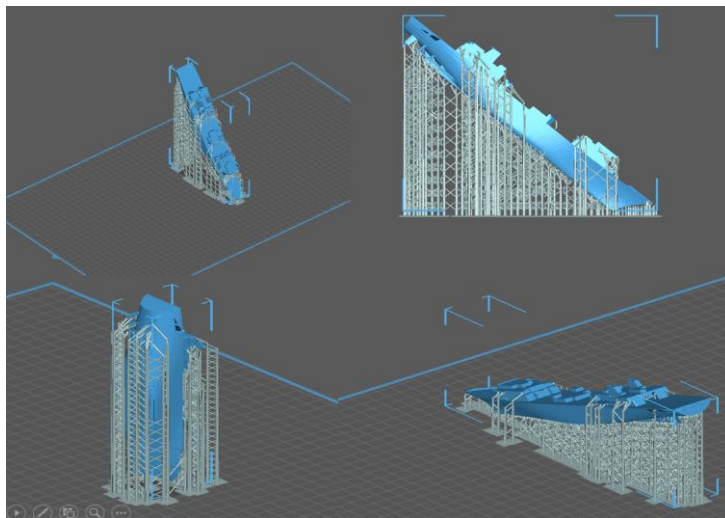


Figure 7. Models and Support Sections

5.2 Experiments and Statistics

As shown in Figure 7, the blue part is the model part and the white part is the support part. As shown in Fig. 4, the model is placed squarely, and the mass of the model is 43.33g (the printing material is PLA) and the mass of the support is 0g; the time needed for forming the model is 87 minutes. Place the model as shown in Fig. 5, where the total mass is 59.32g and the supporting mass is 15.99g; the time taken to form the model is 201 minutes. The model is positioned at an angle to the printing plate as illustrated in Fig. 6, with the angle marked as the angle between the two red lines in the figure, denoted as θ . The mass of the

model, the mass of the support, and the time required for forming the model with different values are provided in the table 4 below:

Table 4. K=1/800 model data

θ	Total mass	Mass of the support	T
0°	43.33 g	0 g	87 min
10°	69.24 g	25.91 g	182 min
12°	73.92 g	30.59 g	201 min
15°	78.60 g	35.27 g	222 min
18°	78.01 g	34.68 g	188 min
20°	79.13 g	35.8 g	186 min
25°	83.89 g	40.46 g	203 min
28°	82.77 g	39.44 g	209 min
30°	83.74 g	40.41 g	216 min
35°	50.37 g	7.04 g	159 min
45°	50.34 g	7.01 g	164 min
60°	54.83 g	11.5 g	187 min
75°	58.02 g	14.69 g	210 min
80°	59.56 g	16.23 g	211 min
90°	59.32g	15.99g	207min

5.3 Plotting and Analysing Line Graphs

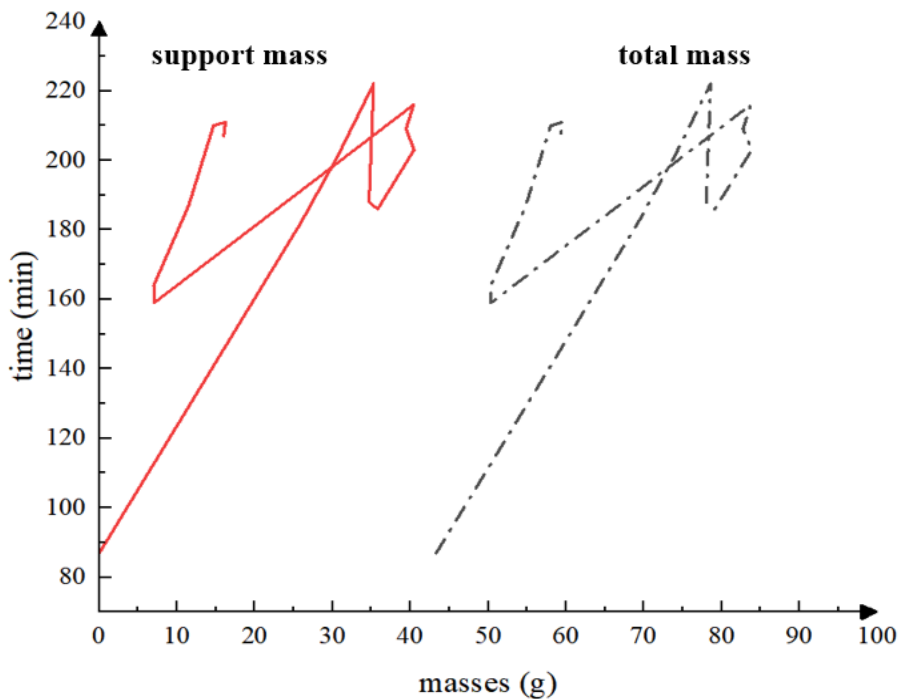


Figure. 8. Relationship between total mass, support mass and forming time

In Figure 8, the mass is plotted against the formation time of the model based on tabular data. Here, the horizontal axis represents mass, while the vertical axis represents time. The red dashed line represents the relationship between support mass and formation time, and the

black dashed line indicates the relationship between total mass and formation time. When the time is fixed, the difference between the two values on the horizontal axis is 43.33. From the two lines, it can be observed that the forming time is directly proportional to the mass within a small range, although there may be two proportional relationships within the same range. There is no obvious pattern between the forming time and the support mass or the total mass of the model as a whole. This suggests that other factors [27] influence the forming time, and the proportion is sometimes greater than that of the mass.

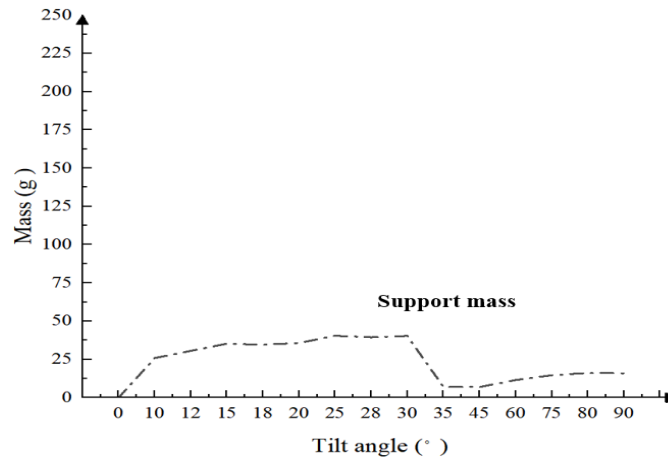


Figure 9. Relationship between tilt angle and support mass

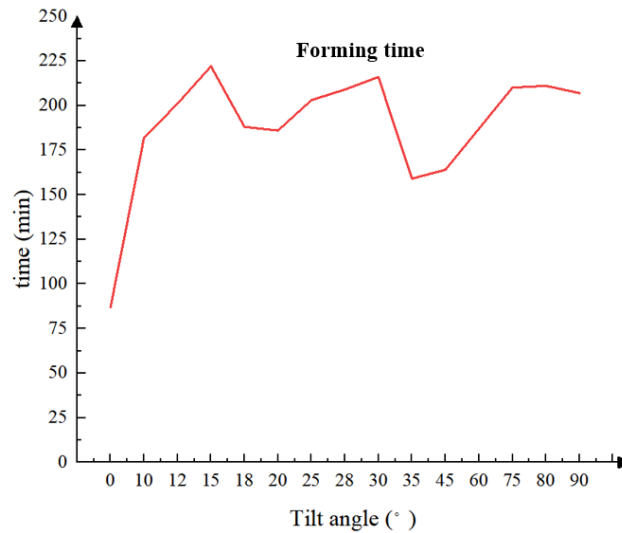


Figure 10. Relationship between tilt angle and forming time

Figures 9 and 10 depict the relationship between tilt angle and support mass, and tilt angle and moulding time, respectively, based on the data in Table 4; as can be seen from the two lines on the graphs, both the support mass and the forming time are positively proportional to the tilt angle in the range of (0°, 10°), with a relatively large rate of change.

At $\theta = (10^\circ, 30^\circ)$, the increase in support mass occurs gradually with the rising tilt angle, showing a relatively steady change. Meanwhile, the forming time initially decreases, then increases with the tilt angle, suggesting a non-linear relationship. Forming time appears to be directly proportional to the tilt angle from approximately $\theta = 20^\circ$ onwards. At $\theta = (30^\circ, 35^\circ)$,

both parameters exhibit an inverse relationship with the angle of inclination, displaying similar slopes and higher rates of change. Between $\theta = (35^\circ, 90^\circ)$, the support mass increases gradually with the tilt angle, while the forming time experiences a rapid increase. Beyond $\theta > 75^\circ$, the rate of increase in forming time shifts from rapid to slow. From the data in the graph we can only conclude that the print time and support quality is minimised when $\theta = 0^\circ$.

5.4 Separate Printing (FDM)

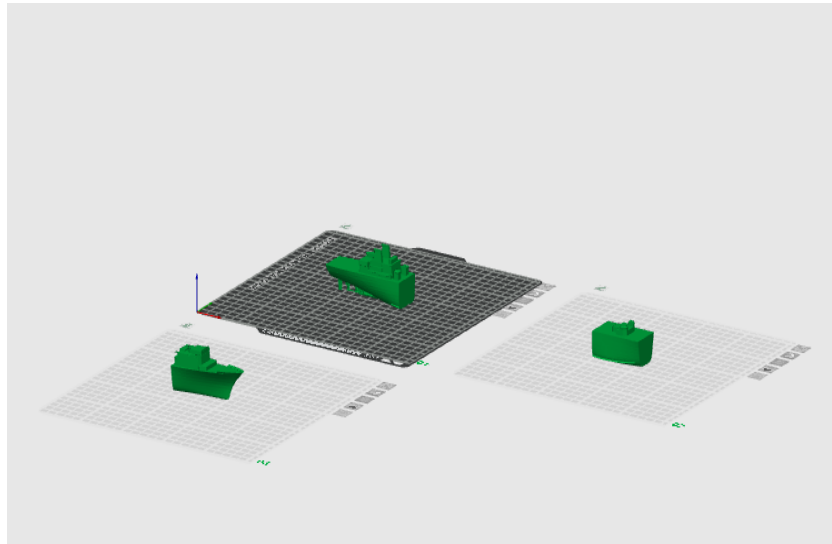


Figure. 11. Parts A, B and C

As depicted in Figure 11, parts A, B, and C are positioned squarely in the print tray, without the addition of any support or rotation. The quality and printing time of each part are detailed in Table 5:

Table 5. K=1/800 model A, B and C data

Model parts	M	Printing time
A	19.67 g	52 min
B	13.05 g	31 min
C	12.23 g	36 min

The combined mass of the three parts is 44.95g, which is 1.62g more than that of the original model. Additionally, the printing time for these parts totals 119 minutes, indicating an increase of 32 minutes compared to the original model. Consequently, segment printing results in a 40% increase in printing time compared to printing the original model as a whole. Whether to opt for segmented printing should be determined by specific circumstances. For instance, if the printed model surpasses the printer's capacity or if additional parts such as electronic components need to be incorporated into a section of the finalized model.

5.4.1 Set the Tilt Angle = 90°

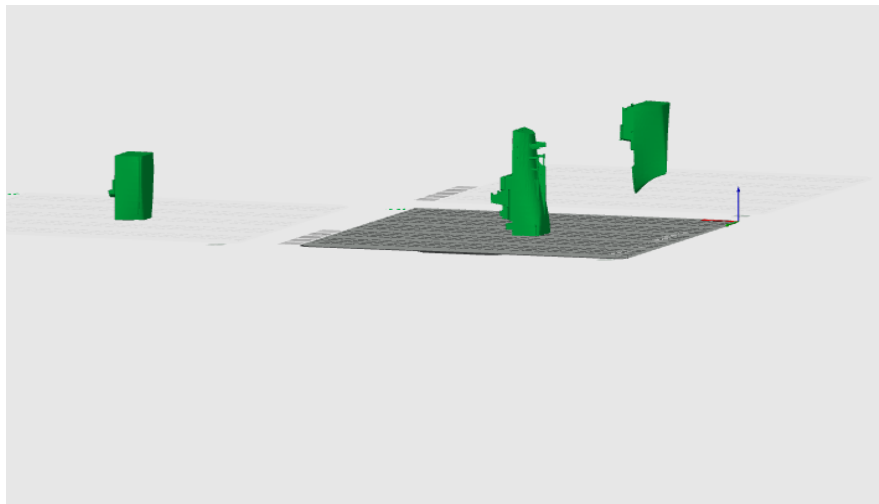


Figure. 12. $\theta = 90^\circ$

After configuring the tilt angle as depicted in Fig. 12, the support mass and printing time for each part of the model are presented in the subsequent table. The variation in printing time compared to the unsupported model is detailed in Table 6 below:

Table 6. Support mass, forming time and time difference

Model parts	Support mass	Printing time	Time difference
A	2.51 g	87 min	35 min
B	0.74 g	46 min	15 min
C	4.86 g	68 min	32 min

The cumulative printing time for the three sections amounts to 219 minutes, with a combined support mass of 8.11g. In contrast, the original model tilted at a 90-degree angle requires 207 minutes of printing time, with a support mass totaling 15.99g. While the data confirms that the printing time for the sections remains greater than that for the entire model, the support required is nearly halved.

5.4.2 Set the Tilt Angle of Part A, PartB and Part C $\theta = -90^\circ$

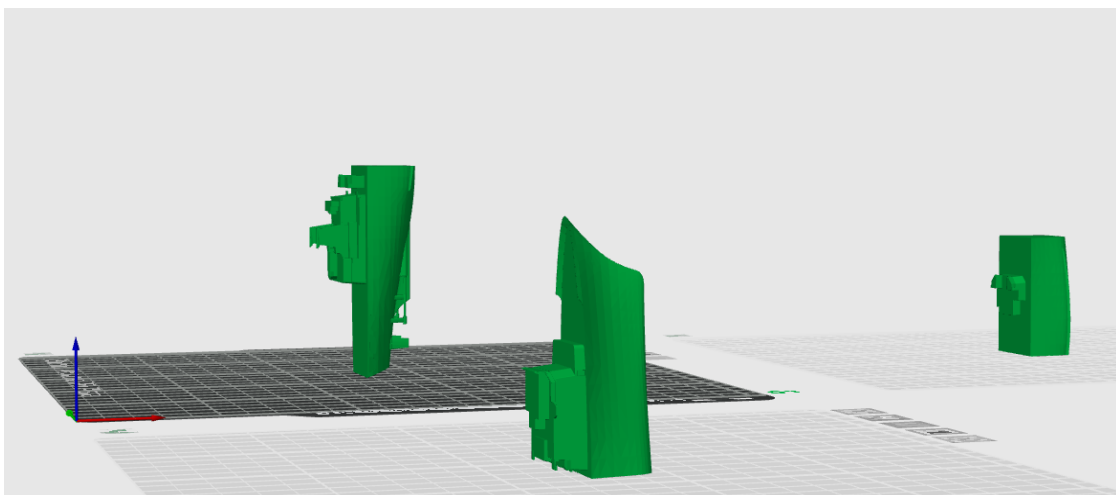


Figure. 13. Cross-section locate on the print plate

Printing time, support mass and other data are shown in the table 7 below :

Table 7. $\theta = -90^\circ$

Model parts	Support mass	Printing time	Time difference
A	6.01 g	93 min	41 min
B	1.12 g	47 min	16 min
C	1.79 g	63 min	27 min

When compared to $\theta=90^\circ$, part A exhibited a nearly 50% reduction in contact area with the print tray, an impressive 139.44% surge in support quality, and a 17.14% augmentation in printing time. On the other hand, part B showed a marginal increase in contact area, accompanied by a 54% enhancement in support quality and a modest 6.06% rise in printing time. In contrast, part C displayed a significant augmentation in contact area with the print tray, but experienced a 63.16% decrement in support quality and a noteworthy 15.62% reduction in printing time. In essence, the model's contact area with the print tray exhibits notable variations, which correlate significantly with both printing time and support quality. Specifically, as the contact area enlarges, the support quality tends to diminish, while the print time shortens.

6. UV-curing 3D printing

6.1 Support Mass in Relation to Print Time

The thickness of each sliced layer is set to 0.2 mm, mirroring that of the FDM printer, while the resin density is established at 1.1 g/ml. The study maintains the deflated model with a deflation coefficient of $K=1/800$ as the focal point, comprising the original model and models A, B, and C. Initially, the deflated original model is employed to examine the correlation between support quantity and printing duration. The approach to adjusting the support quantity remains consistent by modifying the model's placement angle. A range of tilt angles ($\theta = [0^\circ, 10^\circ, 12^\circ, 15^\circ, 18^\circ, 20^\circ, 25^\circ, 28^\circ, 30^\circ, 35^\circ, 45^\circ, 60^\circ, 75^\circ, 80^\circ, 90^\circ]$) is selected, with the model's mass recorded at 121.3g when $\theta=0^\circ$. Altering the placement angle varies the support volume, and the resulting printing times for different support volumes are tabulated in Table 8 below:

Table 8. In light curing, the relationship between tilt angle and support mass, forming time

θ	Support mass	Forming time
0°	0 g	47 min
10°	28.7 g	79 min
12°	29.9 g	84 min
15°	33.7 g	92 min
18°	36.6 g	99 min
20°	39.1 g	104 min
25°	41.6 g	121 min
28°	42.5 g	131 min
30°	41 g	137 min
35°	44.6 g	152 min

45°	42 g	178 min
60°	26.7 g	212 min
75°	26.5 g	236 min
80°	25.1 g	241 min
90°	38.9 g	245 min

6.1.1 Create a Line Graph Illustrating the Relationship Between Support Mass and Print Time

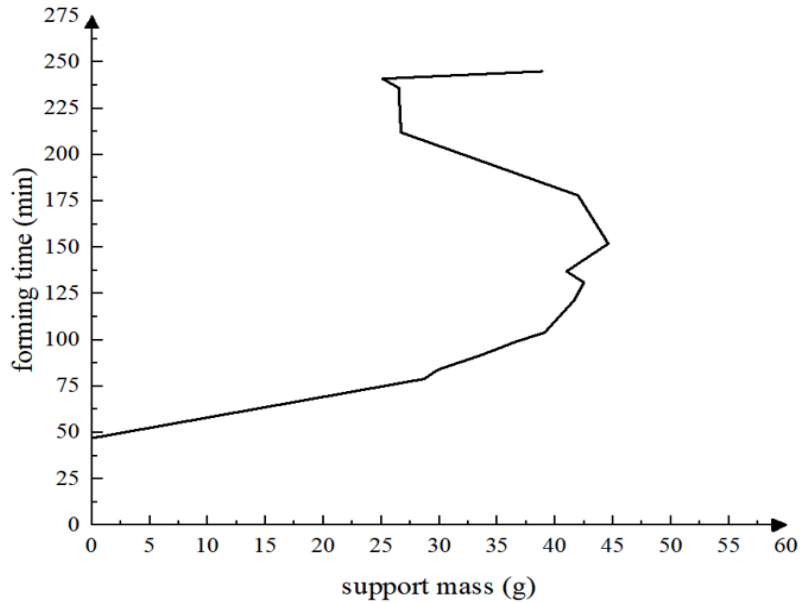


Figure. 14. Graph support mass versus print time

Examining the plot of support mass versus forming time in isolation, during the initial segment of the curve, the support mass shows a proportional relationship with forming time, characterized by a slight slope. However, after $\theta = 40^\circ$, the curve takes on an S-shape, indicating that identical support masses correspond to multiple forming times. In the latter segment, no clear pattern emerges, resembling the scenario observed in the FDM process.

6.1.2 Plot Line Graphs Illustrating the Relationship Between Tilt Angle and Both Support Mass and Print Time.

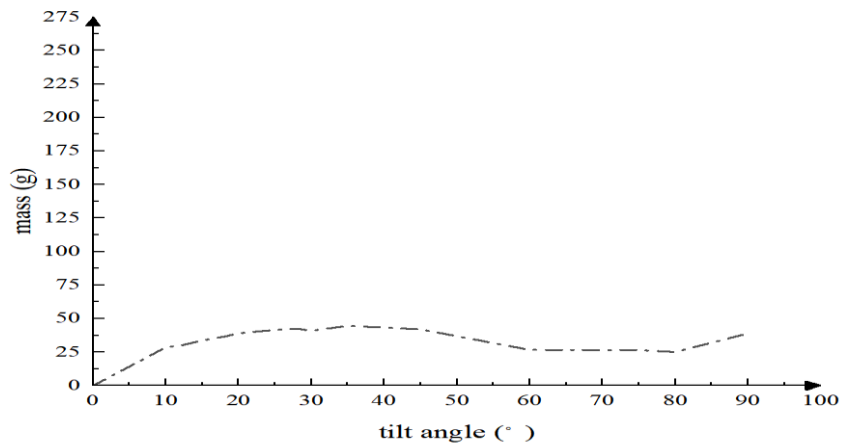


Figure. 15. Graph of tilt angle versus support mass

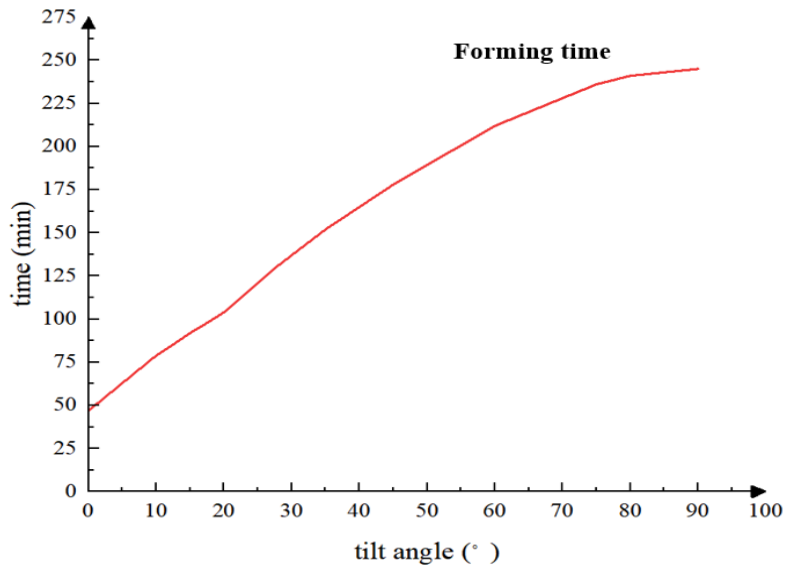


Figure. 16. Graph of tilt angle versus print time

From the figure15, it's evident that the forming time increases as the placement angle rises, displaying a clear positive correlation. Meanwhile, the support mass exhibits a positive correlation within the range of $\theta = (0^\circ, 45^\circ)$, with a steeper increase observed at $\theta = (0^\circ, 10^\circ)$, tapering off gradually thereafter. Notably, it begins to display an inverse proportionality around $\theta = 40^\circ$ and returns to a positive correlation near $\theta = 80^\circ$. These relationships between the placement angle and support mass are depicted in Figure 16. Comparing Figure 9 and Figure 10, it's apparent that the trends in both parameters follow a similar pattern, suggesting a consistent mechanism governing support quality across different software, which is tied to the placement angle.

6.2 Segmented Printing in Light Curing

Set the tilt angle to $\theta=0^\circ$,import the deflated models of parts A, B, and C without support; the mass and forming time data for each part are presented in the table 9 below:

Table 9. Modelling mass and forming time

Model	Model mass	Forming time
A	50.7 g	47 min
B	39 g	35 min
C	31.5 g	43 min

The combined mass of the three parts amounts to 121.2g, which is 0.1g less than the original model. Additionally, the combined forming time for these parts totals 145 minutes, marking an increase of 98 minutes compared to the original model, approximately 208% longer. By consolidating the segmented printing data, it becomes evident that while the total mass of all segmented models remains relatively similar to that of the original model, there's a significant increase in forming time.

7. Conclusions and Recommendations

Based on the experimental data from the two additive manufacturing processes, it's observed that the mass of the support increases as the tilt angle of the model placement varies from 0 to 40 degrees. Beyond 40 degrees, however, the mass begins to decrease initially before rising again. There appears to be no discernible correlation between the support mass and the forming time of the model. In FDM 3D printers, a localized pattern emerges between the tilt angle and forming time, whereas in light-curing 3D printers, the placement angle directly correlates with forming time

When employing both processes for segmented printing, the combined masses of each segment show no significant difference compared to the original unsegmented model. However, there is a significant increase in the forming time of the model. To ensure shorter modeling times and minimize material consumption, the following three recommendations are proposed:

1. Maximize the model within each segment; in other words, reduce the segmentation of the model.
2. The contact area between the model and the printing plate is as large as possible
3. Keep the distance between the print plate and the model's highest point as minimal as possible
4. Avoiding material concentration in 3D printing affects the surface quality of the model.

The inclination angle $\theta = 0^\circ$ of the model in this experiment adheres to the aforementioned three suggestions, effectively minimizing both molding time and support quality. However, excessive material concentration can result in suboptimal texture or even missing details, compounded by the "staircase effect" [28]. In such cases, it becomes necessary to adjust the model's placement angle accordingly. Having accurate data on all aspects of manufacturing a part can be very useful in saving costs and time, for example, offshore facilities vary in size and shape and each offshore facility requires specific design and testing [29]. For further insights into the structural integrity of the final print and guidance on designing segmented print structures effectively, readers can explore resources on ship structural strength design [30-31] or consult a local expert in the field.

Acknowledgments: I am very sincerely grateful to Dr. Dapeng Zhang for his guidance and direction of my research; I am also grateful to Yi Zhang and Yining Zhang for pointing out the errors in my article and guiding the revision so that we can have a higher quality article, and I am also grateful to Yifan Xie for his help with the technique and instrumentation; I am very grateful to the various people for their help!

Funding: This work was financially supported by Program for Scientific Research Start-up Funds of Guangdong Ocean University(grant number 060302112008) and the National Natural Science Foundation of China(grant number 62272109) .

Conflict of interest: The authors of the article have consulted with each other and have no conflict of interest.

References:

- [1] Bikas, Harry, Panagiotis Stavropoulos, and George Chryssolouris. "Additive manufacturing methods and modelling approaches: a critical review." *The International Journal of Advanced Manufacturing Technology* 83 (2016): 389-405.
- [2] Dilberoglu, Ugur M., et al. "The role of additive manufacturing in the era of industry 4.0." *Procedia manufacturing* 11 (2017): 545-554.
- [3] Li, Mengzhen, C. Guedes Soares, and Renjun Yan. "Free vibration analysis of FGM plates on Winkler/Pasternak/Kerr foundation by using a simple quasi-3D HSDT." *Composite Structures* 264 (2021): 113643.
- [4] Qiu, Yu, et al. "An improved numerical method for calculating mechanical properties of bi-modulus sandwich composite structures." *Ocean Engineering* 250 (2022): 110998.
- [5] Zhang Y, Zhang D, Jiang H. A review of artificial intelligence-based optimization applications in traditional active maritime collision avoidance[J]. *Sustainability*, 2023, 15(18): 13384.
- [6] Meng Ling adolescent. On the application of 3D printing in the field of shipbuilding[J]. *China Equipment Engineering*,2020(07):193-194.(in Chinese)
- [7] Liang Z., Si K., Xie Y., Lin Q., Zhao G., Zhang Y. A Study of Small-Scale Aircraft Carrier Modelling in Educational Practice. *Eng. Solut. Mech. Mar. Struct. Infrastruct.*, 2024, 1(2).
- [8] MEI Menglei, QIN Qi, FANG Xinyue, et al. Introduction to the application of 3D printing technology in the field of ships[J]. *Guangdong Shipbuilding*, 2023, 42(06): 70-72+77. (in Chinese)
- [9] Chang, Kuang-Hua. *Motion Simulation and Mechanism Design with SOLIDWORKS Motion 2024*. SDC publications, 2024.
- [10] Bethune, James D. *Engineering Design and Graphics with SolidWorks 2019*. Macromedia Press, 2019.
- [11] Mamajonova, Nodira, et al. "Exploring the Possibilities of 3DS MAX in Architectural Design: A Comprehensive Review." *HOLDERS OF REASON* 2.1 (2024): 383-391.
- [12] Patil, Sonali, Yogesh Deshpande, and Dattatraya Parle. "Extracting Slicer Parameters from STL file in 3D Printing." *International Journal of Intelligent Systems and Applications in Engineering* 12.14s (2024): 192-204.
- [13] Lee, Ching Hao, et al. "Potential for natural fiber reinforcement in PLA polymer filaments for fused deposition modeling (FDM) additive manufacturing: A review." *Polymers* 13.9 (2021): 1407.
- [14] Awasthi, Pratiksha, and Shib Shankar Banerjee. "Fused deposition modeling of thermoplastic elastomeric materials: Challenges and opportunities." *Additive Manufacturing* 46 (2021): 102177.
- [15] Shichong, W. A. N. G., et al. "Development and applications of UV-curing 3D printing and photosensitive resin." *Journal of Functional Polymers* 35.1 (2022): 19-35.
- [16] Kim, Ye Chan, et al. "UV-curing kinetics and performance development of in situ curable 3D printing materials." *European Polymer Journal* 93 (2017): 140-147.

- [17] Wang Shichong, Zhu Yuwei, Wu Yao, et al. Development and application of light-curing 3D printing technology and photosensitive resin[J]. *Journal of Functional Polymers*, 2022, 35(01):19-35. (in Chinese)
- [18] Dogan, Mustafa Doga, et al. "G-ID: identifying 3D prints using slicing parameters." *Proceedings of the 2020 CHI Conference on Human Factors in Computing Systems*. 2020.
- [19] Zhang, Yi, Dapeng Zhang, and Haoyu Jiang. "Review of Challenges and Opportunities in Turbulence Modeling: A Comparative Analysis of Data-Driven Machine Learning Approaches." *Journal of Marine Science and Engineering* 11.7 (2023): 1440.
- [20] Zhang, Y, Xie, Y., Zhao, G., Liang, Z., Shi, J., and Yang, Y. "The Important Role of Fluid Mechanics in the Engineering Field." *Mechanics* 9 (1977): 421-445.
- [21] Zhang, D., Zhao, B., Zhang, Y., and Zhou, N. "Numerical simulation of hydrodynamics of ocean-observation-used remotely operated vehicle." *Frontiers in Marine Science* 11 (2024): 1357144.
- [22] Cao Yali. Research on the accuracy of 3D printing slicing software[J]. *Screen Printing*, 2023(14):91-93. (in Chinese)
- [23] Zhang, Duan Zhong, Jiajia Waters, and Paul Linford Barclay. Material point generation from an STL file. No. LA-UR-22-30587. Los Alamos National Laboratory (LANL), Los Alamos, NM (United States), 2022.
- [24] Kumar, Ajay, et al. "Printing file formats for additive manufacturing technologies." *Advances in Additive Manufacturing* (2023): 87-102.
- [25] Wüthrich, Michael, et al. "A novel slicing strategy to print overhangs without support material." *Applied Sciences* 11.18 (2021): 8760.
- [26] Tricard, Thibault, Frédéric Claux, and Sylvain Lefebvre. "Ribbed support vaults for 3D printing of hollowed objects." *Computer Graphics Forum*. Vol. 39. No. 1. 2020.
- [27] Singh, Jatinder, et al. "Influence of process parameters on mechanical strength, build time, and material consumption of 3D printed polylactic acid parts." *Polymer Composites* 43.9 (2022): 5908-5928.
- [28] Haidiezul, A. H. M., A. F. Aiman, and B. Bakar. "Surface finish effects using coating method on 3D printing (FDM) parts." *IOP Conference Series: Materials Science and Engineering*. Vol. 318. IOP Publishing, 2018.
- [29] Zhang, Yi, Dapeng Zhang, and Haoyu Jiang. "A review of artificial intelligence-based optimization applications in traditional active maritime collision avoidance." *Sustainability* 15.18 (2023): 13384.
- [30] Chen, Diyi, et al. "Research on Structural Strength of Different Car Ro-Ro Ships by Comparison Between Flexible and Rigid Deck Designs in Upright Condition." *ISOPE International Ocean and Polar Engineering Conference*. ISOPE, 2018.
- [31] Chen, Diyi, et al. "Research on Structural Strength of Different Car Ro-Ro Ships by Comparison Between Flexible and Rigid Deck Designs in Upright Condition." *ISOPE International Ocean and Polar Engineering Conference*. ISOPE, 2018.